Title

Subchondral insufficiency fractures of the femoral head: associated imaging findings and predictors of clinical progression

Journal

European Radiology, 26(6)

ISSN

0938-7994

Authors

Hackney, Lauren A
Lee, Min Hee
Joseph, Gabby B
et al.

Publication Date

2016-06-01

DOI

10.1007/s00330-015-3967-x

Peer reviewed

Eur Radiol
DOI 10.1007/s00330-015-3967-x

MUSCULOSKELETAL

Subchondral insufficiency fractures of the femoral head: associated imaging findings and predictors of clinical progression

Lauren A. Hackney[1] · **Min Hee Lee**[1,2] · **Gabby B. Joseph**[1] · **Thomas P. Vail**[3] · **Thomas M. Link**[1]

Received: 3 April 2015 / Revised: 11 June 2015 / Accepted: 5 August 2015

Abstract

Objectives To characterize the morphology and imaging findings of femoral head subchondral insufficiency fractures (SIF), and to investigate clinical outcomes in relation to imaging findings.

Methods Fifty-one patients with hip/pelvis magnetic resonance (MR) images and typical SIF characteristics were identified and reviewed by two radiologists. Thirty-five patients had follow-up documentation allowing assessment of clinical outcome. Subgroup comparisons were performed using regression models adjusted for age and body mass index.

Results SIF were frequently associated with cartilage loss (35/47, 74.5 %), effusion (33/42, 78.6 %), synovitis (29/44, 66 %), and bone marrow oedema pattern (BMEP) (average cross-sectional area 885.7±730.2 mm^2). Total hip arthroplasty (THA) was required in 16/35 patients, at an average of 6 months post-MRI. Compared to the THA cohort, the non-THA group had significantly ($p<0.05$) smaller overlying cartilage defect size (10 mm vs. 29 mm), smaller band length ratio and fracture diameters, and greater incidence of parallel fracture morphology ($p<0.05$). Male gender and increased age were significantly associated with progression, $p<0.05$.

Conclusions SIF were associated with synovitis, cartilage loss, effusion, and BMEP. Male gender and increased age had a significant association with progression to THA, as did band length ratio, fracture diameter, cartilage defect size, and fracture deformity/morphology.

Key points

- *Femoral head subchondral insufficiency fractures (SIF) frequently require total hip arthroplasty (THA).*
- *SIF frequently coexist with synovitis, cartilage loss, and bone marrow oedema pattern.*
- *SIF cartilage defect size, band length ratio, and fracture diameter/morphology can predict progression risk.*

Keywords Femoral head · Insufficiency fracture · Subchondral fracture · Magnetic resonance imaging · Total hip arthroplasty

Abbreviations

BMEP	Bone marrow oedema pattern
ICC	Intraclass correlation
JSN	Joint space narrowing
KL	Kellgren–Lawrence
OARSI	Osteoarthritis Research Society International
SIF	Subchondral insufficiency fracture of the femoral head
THA	Total hip arthroplasty

Introduction

Subchondral insufficiency fractures of the femoral head (SIF) were first described in 1996 by Bangil et al. who used magnetic resonance (MR) imaging and bone scintigraphy to confirm the diagnosis [1]. Previously thought to be a disease predominantly

✉ Lauren A. Hackney
lhackney@montefiore.org

[1] Department of Radiology and Biomedical Imaging, University of California, San Francisco, 185 Berry Street, Suite 350, San Francisco, CA 94107, USA

[2] Department of Radiology and Research Institute of Radiology, Asan Medical Center, University of Ulsan College of Medicine, Seoul, Korea

[3] Department of Orthopaedic Surgery, University of California, San Francisco, CA, USA

Published online: 03 September 2015

affecting elderly patients, SIF have since been reported in adults of varying ages and activity levels [2–4]. Though subchondral fractures do not necessarily comprise a separate disease process, SIF have been identified as a separate entity from osteonecrosis and trauma-related subchondral fractures through histopathologic evaluation [5, 6]. Several authors have also proposed a distinction in the natural history for these lesions [7, 8]. With improvements in MR imaging quality over the last 20 years, multiple studies have allowed radiologists to characterize precise imaging characteristics of this type of fracture, including a discrete low-intensity band on T1-weighted imaging that corresponds to the associated fracture and repair tissue [5, 9, 10]. The imaging characteristics setting this pathology apart from osteonecrosis of the femoral head are quite subtle but have been well described in the literature and include differences in fracture morphology, with parallel or serpiginous fracture lines being more characteristic of SIF [11–13].

Though the diagnostic criteria for SIF can be subtle, there may be significant implications for both prognosis and long-term management that highlight the need for diagnostic accuracy. In contrast to subchondral fractures that occur in the setting of femoral head osteonecrosis, SIF have occasionally been shown to resolve with a period of rest and limited weight-bearing [1, 14, 15]. On the other hand, several cases in the literature have shown rapid progression to advanced collapse, necessitating a total hip arthroplasty (THA) [16–18]. Despite this discrepancy in prognosis among those with SIF, little information exists to date that establishes firm criteria linked to progression of these fractures to advanced collapse, though this information would be critical for treatment decisions. Characteristics such as fracture length and band length ratio (defined as the ratio of the fracture line diameter to the entire weight-bearing portion of the femoral head) have been shown in previous studies to be associated with radiographic progression, as has patient age at the time of diagnosis [19, 20]. But to date studies focusing on SIF have been limited by small sample sizes.

We hypothesized that imaging characteristics representing worsened fracture severity would be predictive of SIF clinical progression. The purpose of our study was to characterize the morphology and imaging findings of SIF, and to investigate clinical outcomes in relation to these imaging findings.

Materials and methods

Study population

This study was approved by our institutional review board and was compliant with the Health Insurance Portability and Accountability Act. Informed consent was waived because of the study's retrospective design. A search of the picture archiving and communications (PACS) databases was conducted for hip/pelvis MR images performed between January 2000 and July 2014. The terms "insufficiency fracture", "stress fracture", and "avascular necrosis" were used and 436 patients were identified. Patients with fractures in other locations or with obvious avascular necrosis were excluded. Patients originally misclassified as having avascular necrosis who upon review were found to have SIF were ultimately included. Two patients less than 18 years old were excluded to avoid skeletal immaturity as a confounding factor. Eventually 51 patients with an imaging diagnosis of SIF were identified (Fig. 1). The diagnosis was based on a low-signal-intensity band along the subchondral femoral head with associated bone marrow oedema pattern (BMEP), a criterion which has previously been published [9–11] (Fig. 2). Two board-certified musculoskeletal radiologists (16 and 22 years of experience, respectively) confirmed the diagnosis in all cases.

The electronic medical record was reviewed to determine the clinical course. Twelve patients for whom no follow-up was documented were included in the non-follow-up group, as were four patients in the non-progression group who had less than 6 months of follow-up after initial MR examination. The remaining 35 patients were included for analysis in the progression arm. Records were reviewed to determine whether patients required THA within the follow-up period. Clinical variables such as medical comorbidities, vitamin D level, dual X-ray absorptiometry (DXA) bone mineral density (BMD), and whether patients underwent temporary weight-bearing limitation were also collected (Table 1).

Image acquisition/analysis

All subjects underwent hip/pelvis MR examination at 3 or 1.5 Tesla (GE Healthcare, Milwaukee, WI). The following sequences were analysed: (1) coronal T1-weighted (-w) fast spin echo (FSE) (echo time [TE]/repetition time [TR]/echo train length/section thickness=5–15 ms/500–1000 ms/3/4 mm),

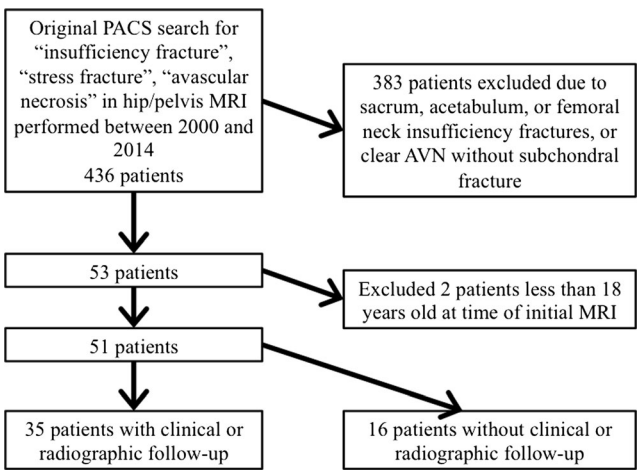

Fig. 1 Flow sheet demonstrating patient selection into follow-up and non-follow-up arms

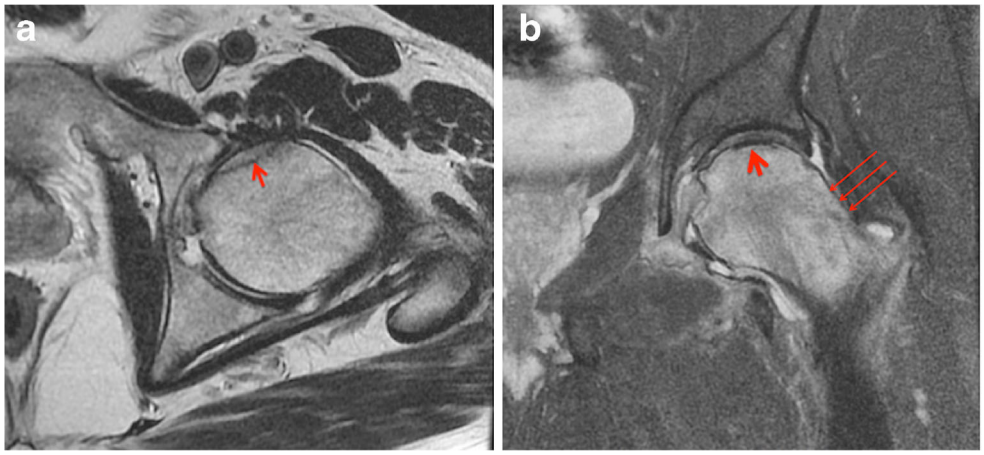

Fig. 2 Subchondral femoral head insufficiency fracture. **a** Axial T1-weighted image demonstrating a low-signal-intensity band extending along the anteromedial portion of the femoral head (*red arrow*). **b** Coronal fat-saturated intermediate-weighted image showing extensive bone marrow oedema pattern throughout femoral head and neck (*thin arrows*); note that the subchondral fracture line can also be appreciated as a hypointense band along the superior subchondral surface (*thick arrow*)

(2) coronal short tau inversion recovery (STIR) (TE/TR/inversion time/flip angle/echo train length/thickness=50–60 ms/3000–9000 ms/150–170 ms/90°/13–18/4 mm), (3) sagittal proton density-w FSE (TE/TR/echo train length/thickness=20–30 ms/1500–4000 ms/8–9/4 mm), (4) sagittal T2-w fat-saturated FSE (TE/TR/echo train length/thickness=50–70 ms/2000–4000 ms/8–16/4 mm), (5) sagittal T1-w FSE (TE/TR/echo train length/section thickness=5–15 ms/500–1000 ms/3/4 mm), and (6) axial T1-w FSE (TE/TR/echo train length/thickness=5–15 ms/500–1000 ms/3/4 mm).

Images were independently graded on PACS workstations (Agfa, Ridgefield Park, NJ) by a board-certified musculoskeletal radiologist and a radiology resident (16 and 2 years experience, respectively), and consensus agreements were used. In cases of disagreement, a third board-certified musculoskeletal radiologist (22 years of experience) was consulted.

Anterior-posterior pelvis and frog-leg lateral radiographs were available for 46 patients. Radiographic variables that were analysed included joint space narrowing (JSN), osteophyte formation, and fracture deformity (Table 2).

Table 1 Demographic characteristics of study

	All subjects (*N*=51)	Non-arthroplasty group (*N*=19)	Arthroplasty group (*N*=16)	*P* value†
Gender*				**0.020**
Male	47.1 (24/51)	36.8 (7/19)	62.5 (10/16)	
Female	52.9 (27/51)	63.2 (12/19)	37.5 (6/16)	
Age^	60±16	56±18	67±11	**0.043**
BMI (kg/m^2)^	27.4±5.6	26.0±4.6	29.6±6.1	0.063
Clinical outcome*			N/A	
Non-THA	54.3 (19/35)			
THA	45.7 (16/35)			
VAS (presentation)^ (25/51)	6.3±2.7	5.6±3.0	7.2±2.4	0.471
Period of non-weight-bearing^				0.407
Yes	23.1 (6/26)	36.4 (4/11)	14.3 (2/14)	
No	76.9 (20/26)	63.6 (7/11)	85.7 (12/14)	
Unknown	9/35	8/19	2/16	
Vitamin D level (ng/mL)^ (19/51)	20±16	29±15	23±14	0.379
Femoral neck BMD^ (17/51)	0.71±0.11	0.659±0.104	0.780±0.098	0.118
Femoral neck T score^ (17/51)	−1.2±1.3	−1.1±1.8	−1.1±0.9	0.404

BMI body mass index, *THA* total hip arthroplasty, *VAS* visual analogue scale, *BMD* bone mineral density

*Values reported as percentages, with number values in parentheses

^Values reported as mean±standard deviation

†Significance defined as $p<0.05$ (see values in bold)

Table 2 Radiographic characteristics of femoral head subchondral insufficiency fractures

	All subjects (*N*=51)	Non-arthroplasty group (*N*=19)	Arthroplasty group (*N*=16)	*P* value†
Joint space narrowing*				0.150
None	45.5 (20/44)	56 (10–18)	7.1 (1/14)	
Mild	22.7 (10/44)	28 (5/18)	28.6 (4/14)	
Moderate	22.7 (10/44)	17 (3/18)	42.9 (6/14)	
Severe	9.1 (4/44)	0	21.4 (3/14)	
Unknown	7/51	1/19	2/16	
Osteophytes*				
None	40.5 (17/42)	44 (8/18)	6.3 (1/16)	0.178
Mild	50 (21/42)	39 (7/18)	68.8 (11/16)	
Moderate	4.8 (2/42)	17 (3/18)	18.8 (3/16)	
Severe	4.8 (2/42)	0	6.3 (1/16)	
Unknown	9/51	1/19	0	
Fracture deformity*				**0.041**
Present	26.1 (12/46)	22 (4/18)	50 (8/16)	
Absent	73.9 (34/46)	78 (14/18)	50 (8/16)	
Unknown	5/51	1/19	0	

*Values reported as percentages, with number values in parentheses

†Significance defined as $p<0.05$ (see value in bold)

Osteophytes were graded as mild, moderate, or severe on the basis of the largest measurable diameter (less than 1 mm, 1–3 mm, or greater than 3 mm, respectively). JSN was similarly graded as mild, moderate, or severe (3–2 mm, 1–2 mm, or less than 1 mm joint space width, respectively). Fracture deformity was defined as loss of femoral head sphericity.

An additional component of our outcomes analysis involved classification of baseline and follow-up radiographs based on Kellgren–Lawrence (KL) grade and Osteoarthritis Research Society International (OARSI) JSN scores. Baseline and follow-up radiographs were graded as KL 0—no radiographic features of OA, 1—doubtful JSN, 2—definite osteophytes and possible JSN, 3—multiple osteophytes, definite JSN and sclerosis, and 4—large osteophytes, marked JSN, severe sclerosis and deformity [21]. Each radiograph was similarly graded on the basis of the OARSI JSN classification as none, mild, moderate, or severe (0–3, respectively) [22, 23]. Progression in either KL or OARSI score was defined as any increase from baseline value.

MR characteristics that were assessed included BMEP cross-sectional area, fracture diameter (coronal and sagittal) and morphology, as well as morphological findings such as muscle atrophy, effusion, and synovitis (Table 3). Fracture location was characterized by dividing the femoral head into nine sub-regions as demonstrated in Fig. 3. BMEP cross-sectional area was determined by measuring the maximum oedema pattern in two orthogonal planes on the coronal image.

Band length ratio, previously described by Iwasaki et al., was determined by calculating the ratio of the coronal fracture diameter to the diameter of the weight-bearing portion of the femoral head (Fig. 4) [19]. Fracture line morphology was characterized as parallel to the joint surface, convex, or serpiginous (Fig. 5). Effusion was defined as increased synovial fluid causing capsular distension, and it was graded as mild or severe (less than or more than 0.7 cm distension, respectively) [24]. Muscle atrophy was graded as none, mild, or severe according to Goutallier's classification (Grade 0, Grade 1/2, and Grade 3/4, respectively) [25]. Synovitis was defined as synovial thickening with effusion and synovial bands/debris.

After interpretations of initial MR images were performed, subsequent images were reviewed. These images were included for descriptive purposes only.

Statistical analysis

Statistical analyses were performed using Stata/IC Version 13 (StataCorp, College Station, TX). Differences in age and body mass index (BMI) between subjects in the progression and non-progression groups were assessed using linear regression models. Logistic regression models adjusted for age and BMI were used to assess the association between predictor variables and progression to THA (outcome). Fracture diameter groups were additionally compared regarding outcome using a chi-squared analysis. To evaluate inter-reader reproducibility, intraclass correlations (ICCs) were calculated for quantitative variables for a subset of ten randomly selected patients.

In order to validate the use of "progression to THA" as an outcome measure, a sub-analysis was included for both "KL

Table 3 MR characteristics of subchondral femoral head insufficiency fractures

	All subjects (*N*=51)	Non-arthroplasty group (*N*=19)	Arthroplasty group (*N*=16)	*P* value†
Location*				0.574
Anteromedial	17.3 (9/51)	16 (3/19)	18.8 (3/16)	
Anterior	21.2 (11/51)	26 (5/19)	25 (4/16)	
Anterolateral	11.5 (6/51)	0	31.2 (5/16)	
Lateral	9.6 (5/51)	16 (3/19)	0	
Posterolateral	13.5 (7/51)	16 (3/19)	6.3 (1/16)	
Posterior	3.8 (2/51)	0	6.3 (1/16)	
Posteromedial	3.8 (2/51)	5 (1/19)	0	
Medial	3.8 (2/51)	0	6.3 (1/16)	
Central	13.5 (7/51)	21 (4/19)	6.3 (1/16)	
Fracture line diameter (mm)^				
Coronal	23±10	20±6	29±12	**0.037**
Sagittal	23±11	21±8	29±10	**0.044**
Fracture line morphology*				**0.045**
Parallel to joint surface	46 (23/50)	68 (13/19)	18.8 (3/16)	
Convex to joint surface	36 (18/50)	11 (2/19)	50 (8/16)	
Serpiginous to joint surface	18 (9/50)	21 (4/19)	31.2 (5/16)	
Unknown	1/51	0	0	
Bone marrow oedema pattern (mm)^				
Cross-sectional area	885.7±730.2	783±800	1011±461	0.404
Sagittal oedema pattern	27±15	25±16	34±11	0.225
Band length ratio^	0.617±0.264	0.550±0.161	0.782±0.321	**0.046**
Overlying cartilage defect size (mm)^	16±14	10±10	29±12	**0.007**
Ligamentum teres*				0.054
Intact	81.6 (40/49)	89 (16/18)	56.3 (9/16)	
Torn	18.4 (9/49)	11 (2/18)	43.8 (7/16)	
Unknown	2/51	1/19	0	
Effusion*				0.523
Absent	21.4 (9/42)	23 (3/13)	6.7 (1/15)	
Mild	52.4 (22/42)	62 (8/13)	53.3 (8/15)	
Severe	26.2 (11/42)	15 (2/13)	40 (6/15)	
Unknown	9/51	6/19	1/16	
Synovitis*				0.074
Absent	34 (15/44)	54 (7/13)	0	
Present	66 (29/44)	46 (6/13)	100 (16/16)	
Unknown	7/51	6/19	0	
Muscle atrophy*				0.239
Absent	43.8 (21/48)	50 (9/18)	6.7 (1/15)	
Mild	45.8 (22/48)	39 (7/18)	66.7 (10/15)	
Severe	10.4 (5/48)	11 (2/18)	26.7 (4/15)	
Unknown	3/51	1/19	1/16	

*Values reported as percentage, with number values in parentheses

^Values reported as mean±standard deviation

†Significance defined as $p<0.05$ (see values in bold)

progression" and "OARSI JSN progression". For both sub-analyses, the outcome groups (progression and non-progression) were compared using Student's *t* tests for the variables band length ratio, coronal/sagittal fracture diameter, and cartilage defect size. Statistical significance in all analyses was defined as $p<0.05$.

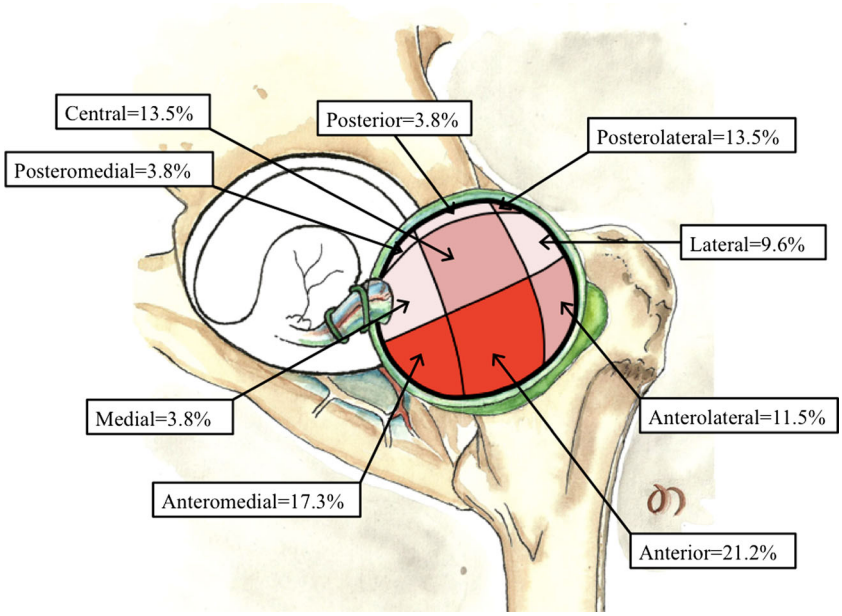

Fig. 3 Classification scheme for location of femoral head insufficiency fracture, as seen from an anteromedial view of the femoral head. Notably, more than one third (38.5 %) of fractures in this study were located in the anteromedial or direct anterior subregions. *Bright red* >15 % of fractures, *dark pink* 10–15 % of fractures, *light pink* <10 % of fractures

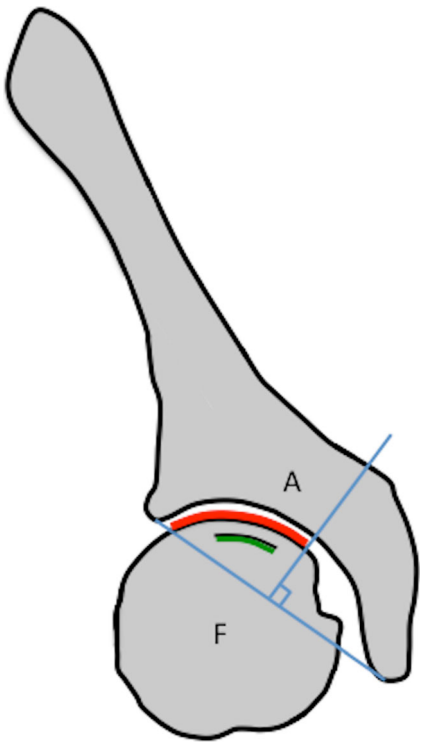

Fig. 4 Method for obtaining band length ratio as described by Iwasaki et al. [19]. A line through the femoral head connecting the lateral edge of the acetabulum to the inferior aspect of the teardrop is drawn, and the weight-bearing portion of the femoral head is defined as the femoral head surface in between the lateral-most aspect of this line, and a perpendicular bisector through the middle of this line. The band length ratio is defined as the ratio of the length of the fracture line at its maximal extent on a coronal image (*green band*) to the weight-bearing portion of the femoral head (*red band*). *A* acetabulum, *F* femoral head

Results

Subject demographics

Demographic and clinical characteristics of the study population are summarized in Table 1. In 35 patients both clinical and imaging follow-up documentation was available; in an additional 16 patients only baseline imaging studies and clinical findings were available (descriptive analysis). Men comprised 24/51 of the study population (47.0 %, mean age 60.1±15.5); women comprised 52.9 % (27/51) of the study population (mean age 60.1±17.3, p=0.992). Of the 35 patients for whom clinical follow-up data were available, 54.3 % (19/35) were treated conservatively (without THA) over an average follow-up of 26.0 months, while 45.7 % (16/35) required THA. Six out of 26 patients (23.1 %) underwent a temporary period of limited weight-bearing as part of their treatment.

Data concerning medical comorbidities was available for 46/51 patients. Four patients (8.7 %) had a history of chronic steroid use, and an equal number had a history of radiation therapy. Three patients (6.5 %) had a history of organ transplant. Vitamin D level was generally low–normal (20±16 ng/mL, normal range 20–50 ng/mL). Femoral neck BMD T scores, which were available for 17/51 patients, were normal (T score at least −1) in 5/17 (29.4 %), osteopenic (T score less than −1 or greater than −2.5) in 10/17 (58.8 %), and osteoporotic (−2.5 or less) in 2/17 (11.8 %).

Baseline radiographic findings

Radiographic and MR characteristics of the entire study population are provided in Tables 2 and 3, respectively. Radiographic

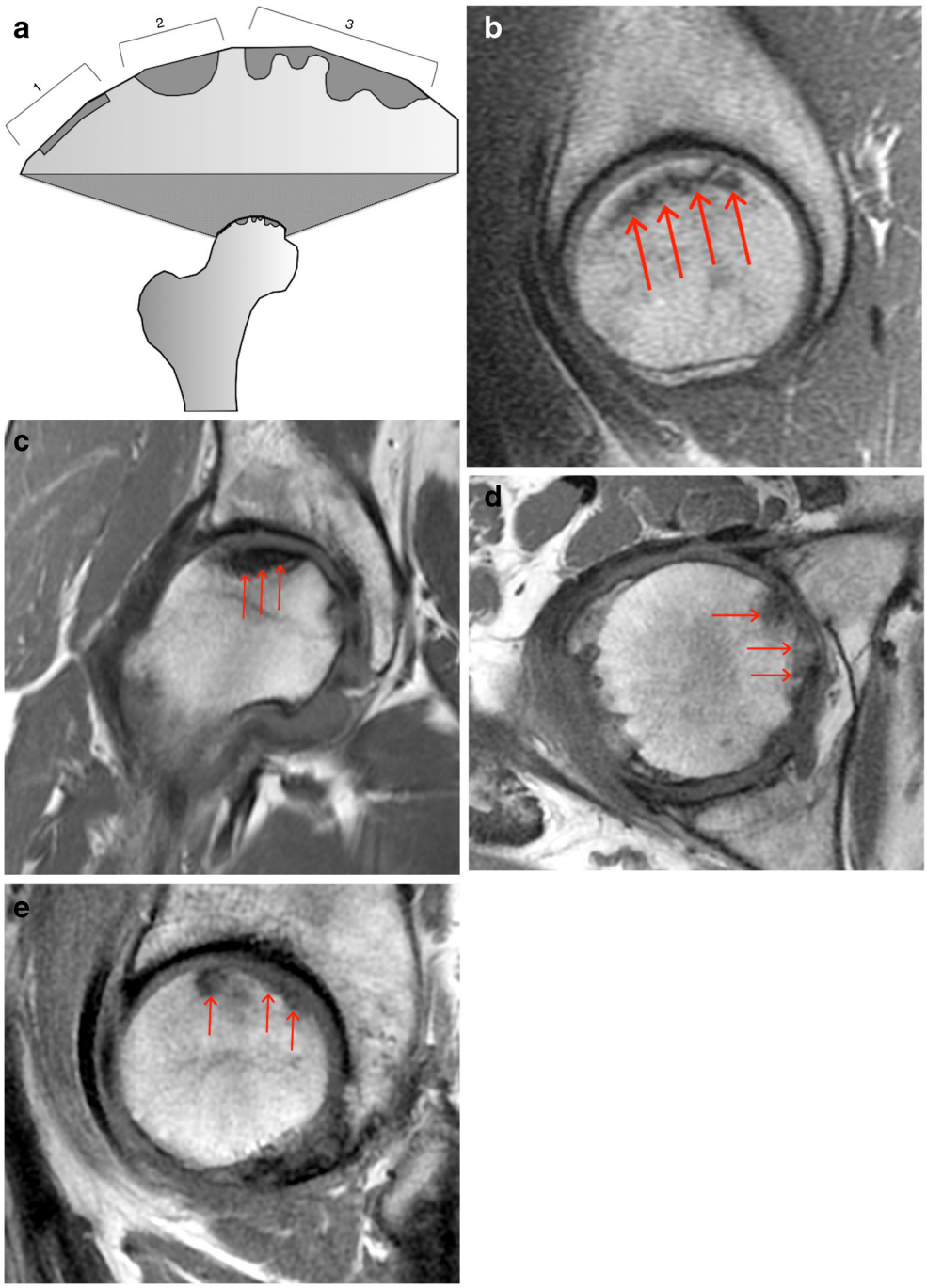

Fig. 5 **a** Schematic image representing the various fracture morphology classifications including parallel (*1*), convex (*2*), and serpiginous (*3*) with respect to the joint surface. **b** T1-weighted sagittal FSE image demonstrating a low-signal-intensity band extending parallel to the joint surface (*red arrows*). **c** T1-weighted coronal FSE image in a different patient demonstrating a subchondral fracture line extending convex to the joint surface (*red arrows*). **d** Axial T1-weighted image in a third patient showing an irregular, serpiginous subchondral fracture line extending along the anteromedial segment of the femoral head (*arrows*). **e** Sagittal T1-weighted image from patient in **d**, again demonstrating the irregular orientation of the fracture line in relation to the joint surface (*arrows*)

findings included JSN in 54.5 % (24/44) and osteophytes in 59.5 % (25/42) of the patients. Twelve of 46 patients (26.1 %) had fracture deformity visualized on initial radiographs.

Baseline MR findings

Roughly two-thirds (64.7 %, 33/51) of fractures were located within the anterior or central portions of the femoral head (Fig. 3); only 21.1 % (11/51) were in the posterior portion of the femoral head. Fracture line diameter was found to measure 23±10 mm on coronal images and 23±11 mm on sagittal images.

Nearly half of fractures were classified as parallel to the joint surface (46 %, 23/50). Extensive BMEP was found in 86.3 % (44/51) with an average cross-sectional area of 885.7±730.2 mm^2, and roughly 37 % (19/51) of patients had a BMEP cross-sectional area greater than 1000 mm^2 (Fig. 2b). Fractures comprised the majority of the weight-bearing portion of the femoral head with an average band length ratio of 0.617±0.264 (Fig. 6a). The majority of patients (35/47,

74.5 %) had some associated cartilage defect, which averaged 16±14 mm in size (Fig. 6b). Labrum (40 %, 20/50) and ligamentum teres (18.4 %, 9/49) tears were relatively infrequent findings, while greater trochanter insertion tendinopathy was present in the majority (76.5 %, 39/51). Findings of surrounding muscle oedema (60.5 %, 26/43), muscle atrophy (56.2 %, 27/48), synovitis (66 %, 29/44), and effusion (78.6 %, 33/42) were also relatively common.

The absolute agreement intraclass correlation coefficients for inter-reader measurement were 0.987 (95 % CI 0.946, 0.997) for BMEP area, 0.905 (95 % CI 0.660, 0.977) for sagittal BMEP, 0.962 (95 % CI 0.854, 0.991) for coronal fracture diameter, 0.982 (95 % CI 0.928, 0.996) for sagittal fracture diameter, 0.945 (95 % CI 0.794, 0.987) for band length ratio, and 0.972 (95 % CI 0.890, 0.993) for cartilage defect size.

Imaging in relation to clinical outcome

In the 35 patients with clinical follow-up, size of the cartilage defect overlying the SIF was found to be significantly associated with progression to THA. Average cartilage defect size in the non-arthroplasty group was 10±10 mm, compared to 29±12 mm in the arthroplasty group, $p<0.001$. This relationship still reached significance when controlling for age and BMI ($p=0.007$). Every 1-mm increase in cartilage defect size resulted in an increased risk of progression to THA of 17.7 % (95 % CI 4.6, 32.4) (Table 3). Interestingly, of the ten patients who had a cartilage defect size less than 10 mm, 10 % progressed to THA (average follow-up 29.7 months), compared to 73.3 % (11/15) of those patients with cartilage defects larger than 20 mm in size (average follow-up 23.2 months).

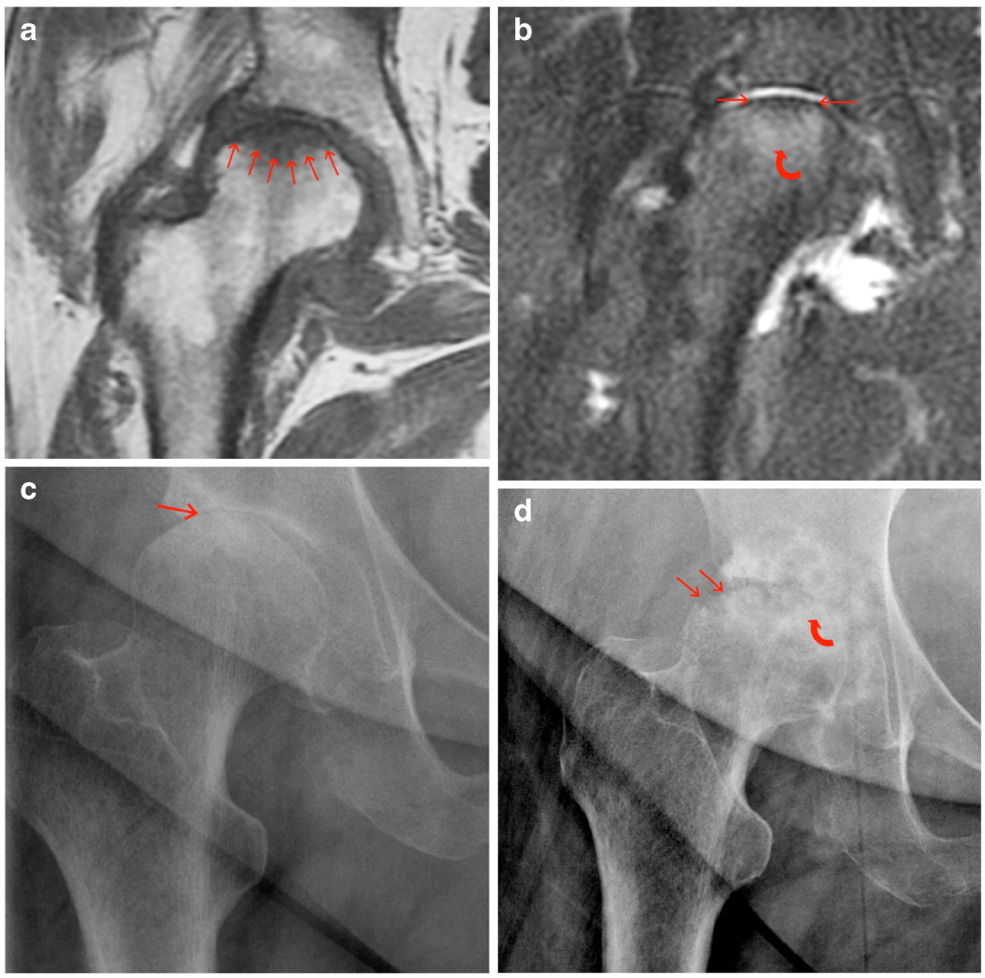

Fig. 6 **a** Coronal T1-weighted FSE image in a 72-year-old obese (BMI 37.3) woman demonstrating a convexly oriented insufficiency fracture (*red arrows*). Band length ratio was measured at 0.811 and fracture diameter was measured at 30 mm. **b** Coronal T2-weighted fat-saturated image showing convex fracture line extending along the subchondral surface of the femoral head, surrounded by extensive bone marrow oedema pattern in the adjacent portions of the femoral head (*curved arrow*). Note the extensive full thickness cartilage loss seen at the superior margin (*straight arrows*). **c** Original anterior-posterior pelvis radiograph taken at same time as initial MR examination. Note that despite significant JSN (*red arrow*) and subchondral sclerosis, there is overall maintenance of femoral head sphericity. **d** Anterior-posterior radiograph of the right hip taken approximately 21 months following the initial radiograph in **c**, showing marked progression of subchondral collapse and loss of femoral head sphericity with cystic changes (*straight arrows*) and worsening sclerosis (*curved arrow*) indicating overall progression of osteoarthritis

Band length ratio was found to be significantly (p=0.046) higher in the arthroplasty group (0.782±0.321) compared to the non-arthroplasty group (0.550±0.160) (Table 3). Similarly, coronal fracture line diameter was found to vary significantly (p=0.037) between the arthroplasty (29±12 mm) and non-arthroplasty (20±6 mm) groups, as was sagittal fracture line diameter (29±10 mm vs. 21±8 mm, respectively, p=0.044). An analysis performed on high and low lesion size groups showed that large coronal fracture diameter (greater than 30 mm) had a significantly increased progression risk compared to the low fracture diameter (less than 20 mm) group (OR 10.0, 95 % CI 1.44, 69.26). An analysis performed for high (greater than 30 mm) and low (less than 20 mm) sagittal fracture diameter groups yielded similar results, with the high diameter group having significantly higher progression risk (OR 15.75, 95 % CI 1.75, 141.40). Fracture morphology also had a significant association (p=0.045) with clinical prognosis, with a parallel morphology more frequently found in the non-progression group.

Radiographic findings such as JSN, osteophyte formation, and radiographic osteopenia were not found to be significantly associated with progression to THA in the study population. However, presence of radiographic fracture deformity was found to be significantly associated with progression to THA (p=0.041) (Table 2).

To validate the use of THA as an outcome measure, sub-analyses involving both KL grade and OARSI JSN scores in defining progression were also performed for band length ratio, coronal and sagittal fracture diameter, and chondral defect size. The results of these sub-analyses were found to correspond appropriately with our main outcomes analysis and are presented in Table 4.

Consideration of clinical predictors

Assessment of the relationship of clinical and demographic variables with regards to progression to THA was also performed, and the results are provided in Table 1. Male gender was significantly associated with progression to THA (p=0.020). Patients in the progression group were also found to be significantly older than patients in the non-progression group (67±11 years vs. 56±18 years, p=0.043). Other clinical parameters such as BMI, BMD/T score of the hip region, vitamin D level, or presence of osteoporosis did not show significant association with progression to THA. Limitation of weight-bearing as therapeutic management seemed to limit progression of SIF, with only 2/6 patients (33.3 %) ultimately requiring THA. However, because of the small sample size, this association did not reach statistical significance.

Progression

A summary of follow-up findings from nine conservatively managed patients is provided in Table 5. Nearly half of these patients had documented improvement of their fracture as assessed on subsequent imaging studies, with improvement of BMEP, resolution of the subchondral fracture line, and, in one case, restoration of femoral head sphericity (Fig. 7). The most common signs of progression included worsening cystic changes and, in one case, visualized progression of cartilage loss with progressive radiographic collapse (Fig. 6).

Discussion

SIF is a relatively new entity with increasing clinical significance, and our study demonstrated morphological imaging abnormalities of SIF as well as criteria associated with increased progression risk. Radiographic fracture deformity and irregular fracture morphology on MR imaging with greater fracture length and cartilage defect size were typically seen with clinical progression of SIF, as were demographic characteristics such as male gender and increased age. To the best of our knowledge this study is the largest to examine both

Table 4 Imaging and demographic variables in relation to radiographic progression

	Non-progression[a] (N=13)	Progression[a] (N=15)	P value†
Band length ratio^	0.511±0.153	0.790±0.330	0.008
Sagittal fracture diameter (mm)^	18.69±7.03	29.60±10.62	0.003
Coronal fracture diameter (mm)^	18.69±5.78	28.80±12.53	0.011
Chondral defect size (mm)^	8.77±8.78	26.20±14.01	0.0005
Age (years)^	55.77±17.96	66.87±10.88	0.067
Male (%, number)	38.5 (5/13)	46.7 (7/15)	0.661

[a] Progression defined as any increase in Kellgren–Lawrence grade or OARSI joint space narrowing score following initial diagnostic image

^Values expressed as mean±standard deviation

†Statistical significance defined as p<0.05

Table 5 Progression on available follow-up imaging

Patient	Age at first MR exam (years)	Gender	Follow-up image type	Time between original and follow-up (months)	Outcome	Details
1	59	Male	XR	20.6	Worsened	Collapse more prominent on follow-up radiograph compared to original. No change in joint space or cartilage remaining
2	18	Female	MR	24.6	Improved	Interval healing of subchondral fracture; no definitive fracture line on follow-up MR images
3	76	Female	XR	12.9	Unchanged	No significant difference compared to original radiograph
4	37	Male	MR	24.4	Unchanged/ improved	Decreased bone marrow oedema pattern, but still with linear fracture line medially
5	28	Male	MR	2.2	Improved	Persistent mild effusion, improved bone marrow oedema pattern, no progression or change of fracture line, improved femoral head morphology (more rounded)
6	72	Female	XR	21.6	Worsened	Significant collapse, more joint space narrowing, more osteoarthritis (cystic changes)
7	70	Female	MR/XR	8.1	Improved	No fracture, no bone marrow oedema pattern, interval spontaneous healing. Mild joint effusion, no muscle oedema but persistent increased signal in gluteal tendon
8	33	Male	MR	5.6	Improved	Improvement in bone marrow oedema pattern. No definitive fracture line
9	41	Female	MR/XR	105.3	Worsened	Progressive sclerosis, subchondral cyst formation. Progression of cartilage loss

XR X-ray, *MR* magnetic resonance

imaging and clinical characteristics of SIF and to determine risk factors for progression.

Our study demonstrates that cartilage defect size is associated with clinical SIF progression. SIF has previously been linked with osteoarthritis development [26]. Niimi et al. suggested that SIF formation is a typical event in the development of rapidly destructive hip osteoarthritis, with biological responses to SIF triggering rapid cartilage breakdown. A similar study confirmed SIF histologically in 11 patients who had experienced rapid JSN of the affected hip over the course of 9 months [16]. Our study confirms these associations between rapidly progressive hip OA and SIF, by demonstrating the relationship between SIF progression and chondral defect size, and by showing the frequent co-occurrence of SIF with radiographic findings of degenerative joint disease in a majority of patients.

Another finding concerns the association of fracture morphology and radiographic deformity with SIF progression. Other studies have investigated potential interpretations of different SIF fracture morphologies [12, 27]. Our study is the first to our knowledge that investigates the influence of fracture morphology on SIF progression, demonstrating that fractures parallel to the joint surface have significantly less progression. This may be attributable to the minimal disruption of the femoral head structural composition associated with parallel fracture morphology. Our study also demonstrated a significant relationship between radiographic deformity and progression. Loss of femoral head sphericity represents increased collapse and instability, and it is not surprising that more destabilized fracture surfaces have higher progression rates. Interestingly, our study did not show a relationship between femoral head BMEP and progression risk. Past studies have suggested that BMEP on MR images can provide insight into the transient nature of some femoral head lesions, and resolution of BMEP over time suggests a reversible lesion [28]. Though our results support the diagnostic utility of BMEP with regards to SIF, they also reiterate BMEP as a non-specific process reflective of a bone marrow stress response and an insignificant predictor of clinical progression.

Our study demonstrated a significant association between coronal fracture diameter and band length ratio with progression risk, confirming results from Iwasaki et al., and also showed that sagittal fracture diameter was significantly associated with progression [19]. Sagittal fracture diameter, which like coronal diameter reflects the extent of injury to the subchondral femoral head surface, should likewise contribute similarly to the stability of this weight-bearing region. Previously published literature had failed to demonstrate this relationship between sagittal fracture diameter/morphology and SIF prognosis, and therefore we feel that our study provides a more through picture of morphologic risk factors for SIF progression. Additionally, by adjusting for age and BMI in a regression model, our study demonstrates that these associations are not purely related to body size variability of SIF patients.

Our study demonstrates a significant relationship between gender and progression, with female patients being less likely

to require THA. This disputes a previous study which demonstrated a *greater* tendency for women with SIF to progress [29]. The basis for this discrepancy is unclear, but may also be related to our multivariate regression model controlling for age and BMI, in addition to small sample sizes in both studies. This study's finding that age and progression risk are significantly associated is not surprising, and it may be confounded by our definition of progression, as older individuals are more likely to be offered THA than a younger cohort. Alternatively, this finding may be a surrogate for more advanced degeneration or longer symptom duration.

In our study, patients treated with a period of weight-bearing limitation at the time of diagnosis had lower rates of SIF progression to THA. This suggests that, in contrast to the natural history of femoral head osteonecrosis, a period of weight-bearing limitation may help to prevent, or slow, SIF progression. Because of a small sample size, our study was not sufficiently powered to detect a difference in progression risk between the weight-bearing and non-weight-bearing groups. Future multi-centre studies may shed light on this new finding of the potential important role of conservative management options in SIF treatment.

Our study has several limitations. The study is limited by its retrospective design and the relatively small number of patients with clinical follow-up. Because our method of patient selection involved a retrospective PACS search, not all patients included in our study had documented clinical or imaging follow-up, presumably because they had undergone follow-up at other institutions or had not sought follow-up at all. Thus, our selected patients had varying degrees of follow-up documentation, and those with limited follow-up may have resulted in underestimation of SIF progression. To limit the potential for such patients to confound our results, we only included patients with limited follow-up (less than 6 months of follow-up in the "non-progression" group) in the descriptive arm of our study. Despite these strict inclusion criteria, to the best of our knowledge this is the largest study to be published.

We also acknowledge our definition of progression as a limitation, due to variability in indications for THA among this population. However, the use of this definition of progression has the benefit of being easily defined and confirmed, and it is generally quite indicative of disease severity; this definition has been used in previous literature in large multi-centre

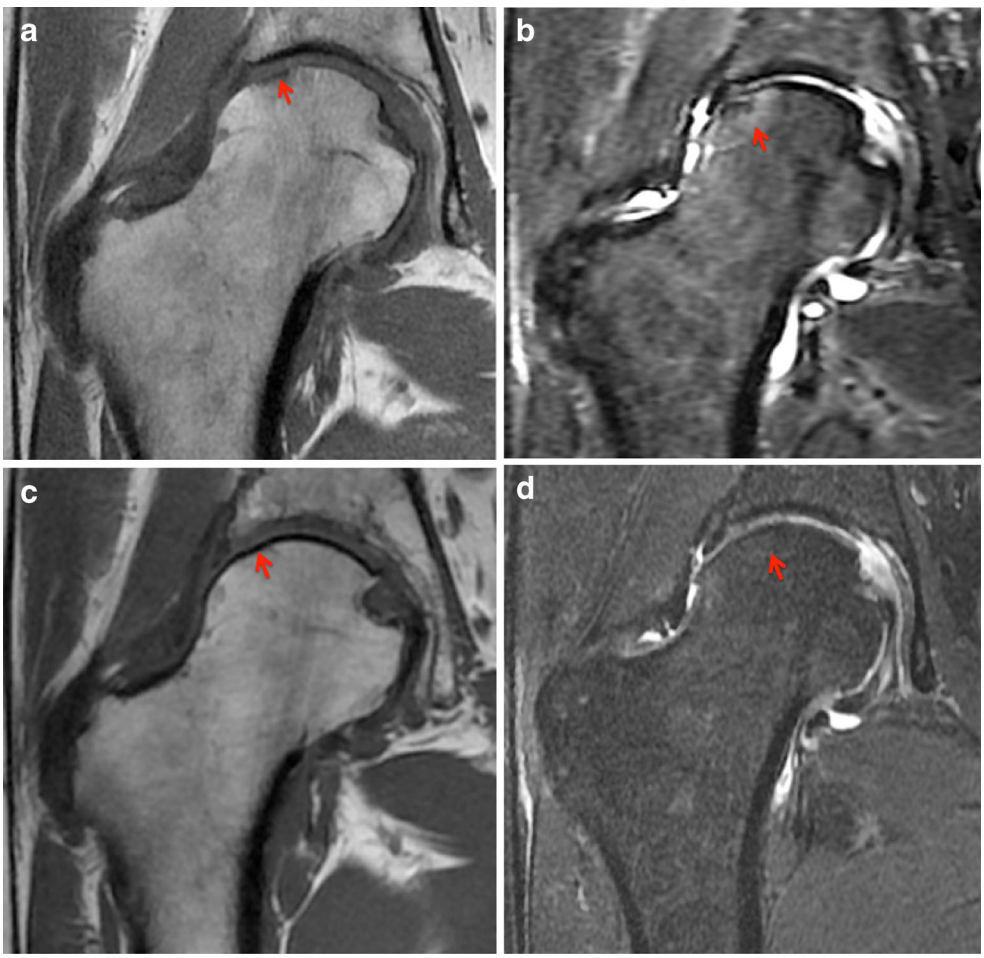

Fig. 7 **a** T1-weighted coronal FSE image showing a hypointense band along the subchondral surface of the superolateral femoral head representing a subchondral insufficiency fracture (*red arrow*). **b** Fat-saturated intermediate-weighted coronal FSE image represents mild amount of bone marrow oedema pattern surrounding the fracture site (*red arrow*). **c** T1-weighted coronal FSE image in the same patient taken 2 months later, after a period of non-weight-bearing, showing near-complete resolution of the fracture line (*red arrow*). **d** Fat-saturated intermediate-weighted coronal FSE image demonstrating resolution of bone marrow oedema pattern (*red arrow*)

trials as a marker for degenerative joint disease progression [4, 20, 29–31]. To further validate the use of this definition of progression, we compared our results of this analysis with those using radiographic definitions of progression, and these have confirmed our significant findings regarding the imaging characteristics associated with worse prognosis.

In conclusion, while nearly half of SIF patients can be treated conservatively; those with larger cartilage defect size, irregular fracture orientation/deformity, or increased band length ratio/fracture diameter have significantly higher rates of progression to THA, as do male and elderly patients. Findings from this study provide pertinent information on the prognosis of patients with SIF and may prove useful in developing an optimal treatment protocol for SIF patients.

Acknowledgments The scientific guarantor of this publication is Dr. Thomas M. Link, MD, PhD, Department of Radiology and Biomedical Imaging, University of California, San Francisco. The authors of this manuscript declare no relationships with any companies whose products or services may be related to the subject matter of the article. This study has received funding by the National Institute of Arthritis and Musculoskeletal and Skin Diseases, a division of the National Institutes of Health, under award number P50AR060752. One of the authors, Gabby B. Joseph, PhD, has significant statistical expertise. Institutional review board approval was obtained. Written informed consent was waived by the institutional review board as a result of the retrospective nature of this study. Methodology: retrospective, diagnostic or prognostic study, performed at one institution.

References

1. Bangil M, Soubrier M, Dubost JJ et al (1996) Subchondral insufficiency fracture of the femoral head. Rev Rhum Engl Ed 63:859–861
2. Iwasaki K, Yamamoto T, Motomura G, Mawatari T, Nakashima Y, Iwamoto Y (2011) Subchondral insufficiency fracture of the femoral head in young adults. Clin Imaging 35:208–213
3. Yamamoto T, Nakashima Y, Shuto T, Jingushi S, Iwamoto Y (2007) Subchondral insufficiency fracture of the femoral head in younger adults. Skelet Radiol 36:S38–S42
4. Yoon PW, Kwak HS, Yoo JJ, Yoon KS, Kim HJ (2014) Subchondral insufficiency fracture of the femoral head in elderly people. J Korean Med Sci 29:593–598
5. Uetani M, Hashmi R, Ito M et al (2003) Subchondral insufficiency fracture of the femoral head: magnetic resonance imaging findings correlated with micro-computed tomography and histopathology. J Comput Assist Tomogr 27:189–193
6. Zhao G, Yamamoto T, Ikemura S et al (2010) A histopathological evaluation of a concave-shaped low-intensity band on T1-weighted MR images in a subchondral insufficiency fracture of the femoral head. Skelet Radiol 39:185–188
7. Yamamoto T, Iwamoto Y, Schneider R, Bullough PG (2008) Histopathological prevalence of subchondral insufficiency fracture of the femoral head. Ann Rheum Dis 67:150–153
8. Yamamoto T, Bullough PG (1999) Subchondral insufficiency fracture of the femoral head: a differential diagnosis in acute onset of coxarthrosis in the elderly. Arthritis Rheum 42:2719–2723
9. Yamamoto T, Schneider R, Bullough PG (2001) Subchondral insufficiency fracture of the femoral head: histopathologic correlation with MRI. Skelet Radiol 30:247–254
10. Davies M, Cassar-Pullicino VN, Darby AJ (2004) Subchondral insufficiency fractures of the femoral head. Eur Radiol 14:201–207
11. Miyanishi K, Hara T, Kaminomachi S, Maeda H, Watanabe H, Torisu T (2009) Contrast-enhanced MR imaging of subchondral insufficiency fracture of the femoral head: a preliminary comparison with that of osteonecrosis of the femoral head. Arch Orthop Trauma Surg 129:583–589
12. Ikemura S, Yamamoto T, Motomura G, Nakashima Y, Mawatari T, Iwamoto Y (2010) MRI evaluation of collapsed femoral heads in patients 60 years or older: differentiation of subchondral insufficiency fracture from osteonecrosis of the femoral head. AJR Am J Roentgenol 195:63–68
13. Ikemura S, Yamamoto T, Motomura G, Nakashima Y, Mawatari T, Iwamoto Y (2013) The utility of clinical features for distinguishing subchondral insufficiency fracture from osteonecrosis of the femoral head. Arch Orthop Trauma Surg 133:1623–1627
14. Rafii M, Mitnick H, Klug J, Firooznia H (1997) Insufficiency fracture of the femoral head: MR imaging in three patients. AJR Am J Roentgenol 168:159–163
15. Hagino H, Okano T, Teshima R, Nishi T, Yamamoto K (1999) Insufficiency fracture of the femoral head in patients with severe osteoporosis: report of 2 cases. Acta Orthop Scand 70:87–89
16. Yamamoto T, Bullough PG (2000) The role of subchondral insufficiency fracture in rapid destruction of the hip joint: a preliminary report. Arthritis Rheum 43:2423–2427
17. Fukui K, Kaneuji A, Fukushima M, Matsumoto T (2015) Early MRI and intraoperative findings in rapidly destructive osteoarthritis of the hip: a case report. Int J Surg Case Rep 8:13–17
18. Yamamoto T, Takabatake K, Iwamoto Y (2002) Subchondral insufficiency fracture of the femoral head resulting in rapid destruction of the hip joint: a sequential radiographic study. AJR Am J Roentgenol 178:435–437
19. Iwasaki K, Yamamoto T, Motomura G et al (2012) Prognostic factors associated with a subchondral insufficiency fracture of the femoral head. Br J Radiol 85:214–218
20. Miyanishi K, Ishihara K, Jingushi S, Torisu T (2010) Risk factors leading to total hip arthroplasty in patients with subchondral insufficiency fractures of the femoral head. J Orthop Surg (Hong Kong) 18:271–275
21. Kellgren J, Lawrence J (1957) Radiologic assessment of osteoarthritis. Ann Rheum Dis 16:494–502
22. Altman RD, Gold GE (2007) Atlas of individual radiographic features in osteoarthritis, revised. Osteoarthr Cartil 15:A1–A56
23. Gossec L, Jordan JM, Lam M et al (2009) Comparative evaluation of three semi-quantitative radiographic grading techniques for hip osteoarthritis in terms of validity and reproducibility in 1404 radiographs: report of the OARSI-OMERACT task force. Osteoarthr Cartil 17:182–187
24. Lee S, Nardo L, Kumar D et al (2014) Scoring hip osteoarthritis with MRI (SHOMRI): a whole joint osteoarthritis evaluation system. J Magn Reson Imaging 41:1549–1557
25. Lippe J, Spang JT, Leger RR, Arciero RA, Mazzocca AD, Shea KP (2012) Inter-rater agreement of the Goutallier, Patte, and Warner classification scores using preoperative magnetic resonance imaging in patients with rotator cuff tears. Arthroscopy 28:154–159
26. Niimi R, Hasegawa M, Sudo A, Uchida A (2005) Rapidly destructive coxopathy after subchondral insufficiency fracture of the femoral head. Arch Orthop Trauma Surg 125:410–413
27. Kubo T, Yamazoe S, Sugano N (1997) Initial MRI findings of nontraumatic osteonecrosis of the femoral head in renal allograft recipients. Magn Reson Imaging 15:1017–1023
28. Vande Berg BC, Malghem JJ, Lecouvet FE, Jamart J, Maldague BE (1999) Idiopathic bone marrow edema lesions of the femoral head: predictive value of MR imaging findings. Radiology 212:527–535

29. Yamamoto T, Karasuyama K, Iwasaki K, Doi T, Iwamoto Y (2014) Subchondral insufficiency fracture of the femoral head in males. Arch Orthop Trauma Surg 134:1199–1203
30. Iwasaki K, Yamamoto T, Motomura G, Ikemura S, Yamaguchi R, Iwamoto Y (2013) Radiologic measurements associated with the prognosis and need for surgery in patients with subchondral insufficiency fractures of the femoral head. AJR Am J Roentgenol 201:W97–W103
31. Bruyere O, Pavelka K, Rovati LC et al (2008) Total joint replacement after glucosamine sulphate treatment in knee osteoarthritis: results of a mean 8-year observation of patients from two previous 3-year, randomised, placebo-controlled trials. Osteoarthr Cartil 16:254–260